Engineering neonatal Fc receptor-mediated recycling and transcytosis in recombinant proteins by short terminal peptide extensions

Jonathan T. Sockolosky, Matthew R. Tiffany, and Francis C. Szoka[1]

Pharmaceutical Sciences and Pharmacogenomics Graduate Program, Department of Bioengineering and Therapeutic Sciences, University of California, San Francisco, CA 94143

Edited by David A. Tirrell, California Institute of Technology, Pasadena, CA, and approved August 17, 2012 (received for review May 24, 2012)

The importance of therapeutic recombinant proteins in medicine has led to a variety of tactics to increase their circulation time or to enable routes of administration other than injection. One clinically successful tactic to improve both protein circulation and delivery is to fuse the Fc domain of IgG to therapeutic proteins so that the resulting fusion proteins interact with the human neonatal Fc receptor (FcRn). As an alternative to grafting the high molecular weight Fc domain to therapeutic proteins, we have modified their N and/or C termini with a short peptide sequence that interacts with FcRn. Our strategy was motivated by results [Mezo AR, et al. (2008) *Proc Natl Acad Sci USA* 105:2337–2342] that identified peptides that compete with human IgG for FcRn. The small size and simple structure of the FcRn-binding peptide (FcBP) allows for expression of FcBP fusion proteins in *Escherichia coli* and results in their pH-dependent binding to FcRn with an affinity comparable to that of IgG. The FcBP fusion proteins are internalized, recycled, and transcytosed across cell monolayers that express FcRn. This strategy has the potential to improve protein transport across epithelial barriers, which could lead to noninvasive administration and also enable longer half-lives of therapeutic proteins.

protein engineering | drug delivery | nanoparticles

It is remarkable that IgG and albumin have exceptionally long plasma half-lives whereas most other human proteins exhibit rapid blood clearance (1). The extended circulation of IgG contributes to the success of antibody therapeutics (2) whereas the rapid clearance of non-IgG proteins limits their therapeutic potential because of the need for frequent injection or continuous infusion. This long half-life of IgG and albumin is a result of interaction with neonatal Fc receptor (FcRn), which creates an intracellular protein reservoir that is protected from lysosomal degradation and subsequently recycled to the extracellular space (3). A number of chemical and recombinant methods have been devised to improve protein half-life. The most common chemical approach, pioneered by Abuchowski et al. in 1977 (4), depends upon the attachment of PEG chains. Although there are numerous Food and Drug Administration (FDA)-approved PEGylated proteins (5), the approach decreases their potency and contributes to their heterogeneity and immunoreactivity. The use of alternative polymers or polymerization strategies addresses these issues (6) but requires additional processing steps to prepare the polymer–protein conjugate. Genetic fusion between a therapeutic protein and either the Fc domain of IgG, albumin, or long, flexible polypeptide extensions (7) has been introduced to extend protein circulation. Fusion to the Fc domain or albumin is a widely adapted strategy to improve protein circulation via a combination of interaction with FcRn and the substantial increase in molecular weight, which reduces renal clearance. Although a number of such fusion proteins are used clinically, the large size of the Fc domain and albumin adversely affects tissue penetration and reduces the specific activity of the fusion partner (8). There have been extensive protein-engineering efforts to overcome these limitations by reducing the size of the Fc domain (9, 10) or albumin (11); however, alternative ligands that target proteins to FcRn have not been explored.

In addition to enabling long circulation, recycling receptors such as FcRn or transferrin expressed in the lung and intestinal epithelia provide a route for transport of protein cargos across the epithelium and into the blood stream (12, 13). A Fc–erythropoietin (Fc–Epo) fusion protein, when administered into the lung in humans, was transported via the FcRn across the lung epithelium (14); however, the Fc–Epo bioavailability is low, perhaps because of the large size of the Fc fusion. Thus, noninvasive protein delivery remains a major challenge (15).

We have devised a strategy for engineering proteins to interact with FcRn through the genetic fusion of a short FcRn-binding peptide (FcBP) sequence to the N and/or C termini of a model fluorescent protein, monomeric Katushka (mKate) (16). We chose FcRn as the molecular target of our engineered proteins because of its ability both to prolong protein circulation and to enable epithelial transcytosis. This approach may overcome limitations associated with chemical modifications, be easy to manufacture, and provide a solution to the rapid elimination and limited protein-delivery routes. As an initial step on the path to more convenient protein delivery, we demonstrate that FcBP fusion proteins can be readily expressed in *Escherichia coli*, exhibit pH-dependent binding to FcRn, and undergo FcRn-mediated recycling and transcytosis.

Results

Protein Expression and Characterization. To test whether proteins genetically modified with a FcBP sequence enable interaction with FcRn, we created *E. coli* expression vectors encoding mKate modified at its *N* and/or *C* termini with FcBP sequences (Fig. 1*A* and Table S1). We chose mKate as a model protein for proof-of-concept studies because of its far-red fluorescent properties, which allow for multifluorophore microscopy studies and simple quantification techniques. The 16 amino acid FcBP gene sequence was fused to the 5′ and/or 3′ end of the gene encoding mKate, separated by a flexible Gly_4Ser linker, and subsequently restriction-cloned downstream of a 5′ polyhistidine tag and thrombin-cleavage site in the pET15b vector. The thrombin site was modified such that cleavage removes the polyhistidine tag, leaving a single glycine residue as the first amino acid followed by the FcBP sequence.

All proteins were adequately expressed in the soluble *E. coli* fraction and, following purification, no significant differences in

Author contributions: J.T.S. and F.C.S. designed research; J.T.S. and M.R.T. performed research; J.T.S. and M.R.T. contributed new reagents/analytic tools; J.T.S. and M.R.T. analyzed data; and J.T.S. and F.C.S. wrote the paper.

The authors declare no conflict of interest.

This article is a PNAS Direct Submission.

[1]To whom correspondence should be addressed. E-mail: szoka@cgl.ucsf.edu.

This article contains supporting information online at www.pnas.org/lookup/suppl/doi:10.1073/pnas.1208857109/-/DCSupplemental.

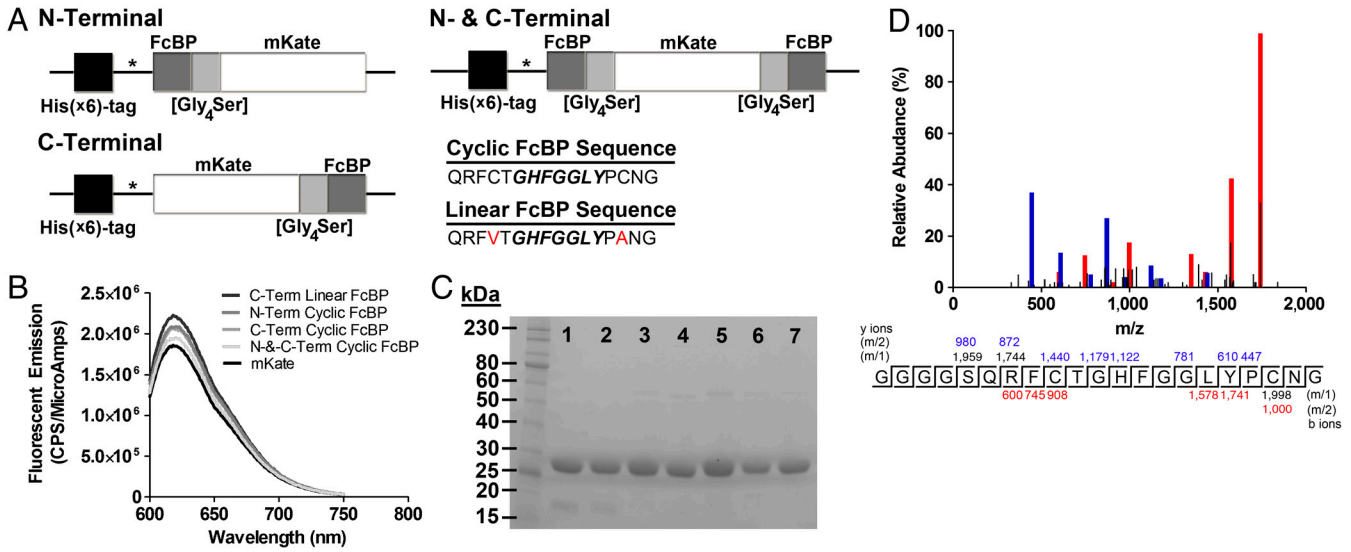

Fig. 1. Construction and characterization of FcBP-modified mKates. (*A*) Diagram of the gene sequences encoding mKate modified at its N and/or C termini with a cyclic or linear FcBP sequence. (*B*) Fluorescence emission spectra comparing equal molar concentrations (500 nM) of mKate (black line) and FcBP-modified mKates (grey lines). (*C*) SDS-PAGE analysis of purified mKate (lane 1), C-Term Linear FcBP mKate (lane 2), C-Term Cyclic FcBP mKate (lane 3), N-Term Cyclic FcBP mKate (lane 4), N-and-C-Term Cyclic FcBP mKate (lane 5), N-and-C-Term Cyclic FcBP mKate Y286H (lane 6), and N-Linear and C-Cyclic FcBP mKate (lane 7). In each lane, 7.5 μg of protein was loaded. (*D*) LC-MS/MS identification of the peptide containing the Gly_4Ser linker and cyclic FcBP sequence from a LysC digest of C-Term Cyclic FcBP mKate. The blue and red peaks correspond to the identified y and b ions, respectively, within the peptide sequence.

fluorescence emission between unmodified and modified mKates were observed (Fig. 1*B*), suggesting that FcBP fusion does not result in major structural changes that disrupt chromophore assembly during protein folding. FcBP fusion results in a subtle change in migration by SDS-PAGE (Fig. 1*C*) from approximately 27 kDa to approximately 30 kDa for mKate and *N*- and *C*-terminal–modified mKates, respectively, in stark contrast to Fc or albumin fusions, which increase molecular mass by approximately 50–70 kDa. Liquid chromatography–tandem mass spectrometry (LC–MS/MS) analysis confirmed expression of mKate modified at its C terminus with a Gly_4Ser linker followed by the cyclic FcBP sequence (Fig. 1*D*).

Binding Kinetics Between FcRn- and FcBP-Modified mKates. We characterized the binding kinetics between FcBP-modified mKate and human FcRn by surface plasmon resonance (SPR). The ability of FcRn to protect IgG from intracellular catabolism is based on two critical properties: pH-dependent binding and bivalency. The interaction between IgG and FcRn occurs at slightly acidic pH (<6.5) with little to no binding at physiological pH. In addition, one IgG molecule contains two FcRn-binding sites, allowing the formation of a 2:1 complex between FcRn and IgG (17). Both properties translate to more efficient binding, recycling, and transcytosis (18), as well as to a longer in vivo half-life of IgG (19), and are important considerations when engineering protein mimetics of the IgG:FcRn interaction. mKate modified with a cyclic FcBP at either its N or C terminus binds FcRn independent of FcBP orientation (N-to-C or C-to-N) with an affinity similar to that reported for the synthetic FcBP (20), indicating that genetic fusion and recombinant expression do not alter its FcRn-binding properties (Table 1). Modification of both the N and C termini of mKate (N-and-C-Term Cyclic FcBP mKate) results in an apparent affinity of 1,023 nM, an approximately 11-fold increase over the single modified mKates, consistent with the role of avidity caused by a bivalent interaction with FcRn. This affinity is comparable to that of hIgG1 at pH 6 ($K_d = 986$ nM by SPR). Unmodified mKate does not bind FcRn, which confirms that binding to FcRn is mediated solely through the FcBP sequence.

We also engineered mKate modified at its C terminus with a linearized FcBP to eliminate potential disulfide heterogeneity within the FcBP sequence. The C-Term Linear FcBP mKate bound FcRn similar to the C-Term Cyclic FcBP mKate, indicating the disulfide is not a requirement for binding to FcRn (Table 1). In addition, a fusion bearing a N-terminal linear and C-terminal cyclic FcBP bound FcRn with an affinity close to that of N-and-C-Term Cyclic FcBP mKate at both pH 6 and pH 7.4 (Table 1 and Fig. S1).

At pH 7.4, binding of all FcBP-modified mKates to FcRn is dramatically reduced compared to pH 6, demonstrating that FcBP fusion confers pH-dependent binding to FcRn (Table 1). However, unlike hIgG1, which has no detectable binding to FcRn at pH 7.4 under the conditions tested, binding of FcBP-modified

Table 1 Binding affinity to human FcRn and in vitro uptake of FcBP modified mKates and hIgG1 in FcRn-expressing MDCK cells

Molecule	FcBP sequence	K_d (SPR)* pH 6, (nM)	K_d (SPR)* pH 7.4, (μM)	$U_{1/2\,max}$ (FACS) pH 6, (nM)	$U_{1/2\,max}$ (FACS) pH 7.4, (μM)
mKate	None	No binding	No binding	No binding	No binding
C-Term Linear FcBP	QRFVT**GHFGGLY**PANG	9,253	154	9,230	>200
C-Term Cyclic FcBP	QRFCT**GHFGGLY**PCNG	14,625	207	14,417	>200
N-Term Cyclic FcBP	QRFCT**GHFGGLY**PCNG	11,290	252	7,077	>200
N-and-C-Term Cyclic FcBP	QRFCT**GHFGGLY**PCNG	1,023	78	814	2.6
N-and-C-Term Cyclic FcBP (Y286H)	QRFCT**GHFGGLH**PCNG	1,480	>1,000	1,529	21.2
N-Term Linear and C-Term Cyclic FcBP	N: QRFVT**GHFGGLY**PANG C: QRFCT**GHFGGLY**PCNG	1,159	148	1,440	2.1
hIgG1	None	986	No binding	1,267	No binding

*Data were fit to a steady-state affinity model for derivation of apparent K_d. SPR data are the mean of two independent experiments.

mKates is detectable by SPR at pH 7.4 (Fig. S2). Because of the low levels of binding, the K_d at pH 7.4 measured by SPR should be viewed as relative and used as a comparator, not as a true affinity.

Cellular Accumulation of FcBP-Modified mKates by Fluorescence-Activated Cell Sorting (FACS). We quantitatively measured cellular accumulation of FcBP-modified mKates in Madin-Darby canine kidney (MDCK) cells stably expressing hFcRn–enhanced YFP (EYFP)/hβ_2m by FACS. Transfected MDCK cells have been widely used as an in vitro model for studying FcRn-mediated endocytosis, recycling, and transcytosis (21). The concentration at which half-maximal uptake ($U_{1/2\,max}$) occurs for each protein was determined by pulsing MDCK hFcRn–EYFP/hβ_2m cells with increasing concentrations of protein at either pH 6 or pH 7.4 and fitting the resulting data to a one-site total binding model in Prism (Fig. 2*A* and Fig. S3). The $U_{1/2\,max}$ values at pH 6 and pH 7.4 correlate with affinity measurements by SPR (Table 1). N-and-C-Term Cyclic FcBP mKate and hIgG1 have a similar $U_{1/2\,max}$ of 814 nM and 1,267 nM, respectively, at pH 6. Taken together with binding affinities measured by SPR, these data demonstrate that mKate modified at both its N and C termini with the cyclic FcBP sequence mimics the IgG:FcRn interaction at pH 6. Cellular accumulation of FcBP-modified mKates and labeled hIgG1 is significantly reduced ($P < 0.001$) when coincubated with excess unlabeled hIgG1 or when incubated at pH 7.4 (Fig. 2*B*), and accumulation in MDCK hβ_2m, wild-type MDCK, and the murine melanoma cell line B16F10 was negligible because of the absence of human FcRn in these cells (Fig. S4).

Because the fluorescent intensity of mKate is pH-dependent (16) we also determined the mean fluorescent intensity (MFI) of mKate in cells in which we clamped the pH at 4.0, 5.0, and 7.4. There is no difference in MFI between mKate-pulsed cells clamped at pH 7.4 compared to cells without ionophore treatment, indicating that the small amount of internalized mKate is not underestimated because of accumulation in low-pH compartments and subsequent loss of fluorescence (Fig. S5). An increase in MFI was observed in N-and-C-Term Cyclic FcBP mKate-pulsed cells clamped at pH 7.4 compared to cells without ionophore treatment (Fig. S5). N-and-C-Term Cyclic FcBP mKate is predominantly localized to FcRn-containing endosomes with an expected pH of approximately 6; therefore, the increase in MFI is consistent with the pH-dependent increase in mKate fluorescence as the pH of the cellular compartments is adjusted to 7.4. Collectively, these FACS data indicate that FcBP-modified mKates interact specifically with FcRn, which facilitates uptake through a FcRn-mediated endocytosis process and is not distorted by nonspecific uptake of the mKate portion of the fusion protein in MDCK hFcRn–EYFP/hβ_2m cells.

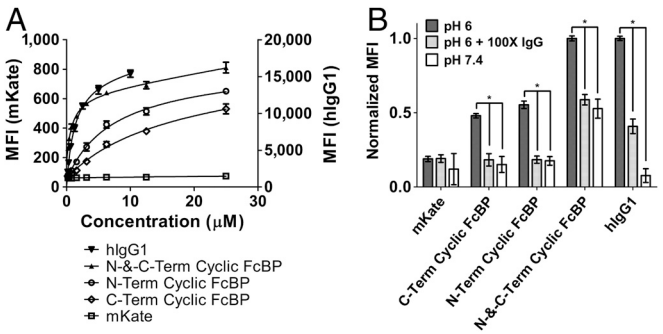

Fig. 2. In vitro characterization of FcBP-modified mKates in MDCK cells expressing hFcRn–EYFP by FACS. (*A*) Cellular accumulation of FcBP-modified mKates and labeled hIgG1 at pH 6 in MDCK hFcRn–EYFP/hβ_2m cells. Solid lines represent data fit to a one-site total binding model in Prism. MFI for mKates and hIgG1 is shown on left and right axes, respectively. (*B*) Cellular accumulation of FcBP-modified mKates and labeled hIgG1 at pH 6 in the presence of 100 mol excess unlabeled hIgG or at pH 7.4. Cells were incubated with 2.5 μM mKate, 2.5 μM mKates modified with a single FcBP, 1 μM N-and-C-Term Cyclic FcBP mKate, or 1 μM labeled hIgG1 with or without 100 mol excess unlabeled hIgG1 as a competitor. The MFI for modified and unmodified mKates was normalized to the maximum MFI for N-and-C-Term Cyclic FcBP mKate. hIgG1 was normalized to itself, given that the fluorescent intensity between the two fluorophores (mKate and TAMRA) are different. Asterisk indicates significance with $P < 0.001$. The data shown in each panel are the mean ($n = 3$), and error bars indicate SD.

Fluorescence Imaging of FcBP-Modified mKates. To understand further the fate of FcBP fusion proteins after internalization we used fluorescence imaging as well as in vitro assays to evaluate FcRn-mediated transport and recycling. The ability of FcRn to salvage protein cargo, particularly IgG, from catabolism initiates in the early endosome (22), where the acidic environment promotes binding to FcRn. FcRn-bound proteins are subsequently trafficked away from the lysosomal pathway (22) and back to the plasma membrane (23), where the elevated extracellular pH results in dissociation from FcRn. Similar to hIgG1, FcBP-modified mKates reside primarily in punctate, endosomal compartments and extensively colocalize with FcRn–EYFP in MDCK cells (Fig. 3*A* and Fig. S6). N-and-C-Term Cyclic FcBP mKate is predominately excluded from lysosomal compartments labeled with either the lysosomal-associated membrane protein 1 (LAMP1) or the lysosomal pathway marker dextran (Fig. 3*B*); however, because of the pH-dependent fluorescence of mKate (16) we cannot exclude the possibility that some lysosomal accumulation occurs but is undetectable because of lysosomal degradation or the reduction of mKate fluorescence in low pH environments (pH < 5). N-and-C-Term Cyclic FcBP mKate not only colocalizes with FcRn–EYFP compartments, but is also trafficked by FcRn–EYFP in a dynamic fashion. A number of well-characterized FcRn–IgG intracellular sorting events (24) are observed between N-and-C-Term Cyclic FcBP mKate and FcRn–EYFP (including full endosomal fusion, vesicle budding, and tubule-mediated transfers; Fig. S7), suggesting that the cellular processing of FcBP-modified cargo has a fate similar to IgG.

Recycling from FcRn-Expressing MDCK Cells. To assess recycling, MDCK hFcRn–EYFP/hβ_2m cells were pulsed with proteins at pH 6 to promote FcRn-dependent internalization of the protein cargo. After removal of noninternalized protein, recycling was determined by measuring the amount of protein returned to the culture medium after a 2-h chase at 37 °C. FcBP-modified mKates are recycled by FcRn in MDCK hFcRn–EYFP/hβ_2m cells, and the amount of recycled protein increases with increasing affinity to FcRn (Fig. 4*A*). Recycling is significantly reduced when incubated at 4 °C ($P < 0.001$), confirming the role of an energy-dependent recycling process. Similarly, recycling is significantly reduced ($P < 0.001$) when pulsed with protein at pH 7.4, a pH that does not favor FcRn-mediated internalization. We also evaluated recycling in MDCK hβ_2m cells, which lack FcRn, and found that in all cases the amount of protein recycled is significantly reduced ($P < 0.001$) when compared to recycling from MDCK hFcRn–EYFP/hβ_2m cells.

Transcytosis Across FcRn-Expressing MDCK Cell Monolayers. Unlike small-molecule drugs, proteins and other large macromolecules are unable passively to cross epithelial barriers because of their large size and hydrophilicity. Therefore, for proteins to penetrate epithelial barriers without disrupting tight junctions, they must be actively transported. FcRn actively transports endogenous IgG across epithelial barriers in the gut and lung. We predicted that FcRn can be hijacked by alternative FcRn-binding cargo, such as FcBP fusion proteins, to enable epithelial transcytosis. N-and-C-Term Cyclic FcBP mKate and hIgG1 are transported from the apical-to-basolateral compartment by FcRn expressed in MDCK hFcRn–EYFP/hβ_2m cells, whereas unmodified mKate is unable

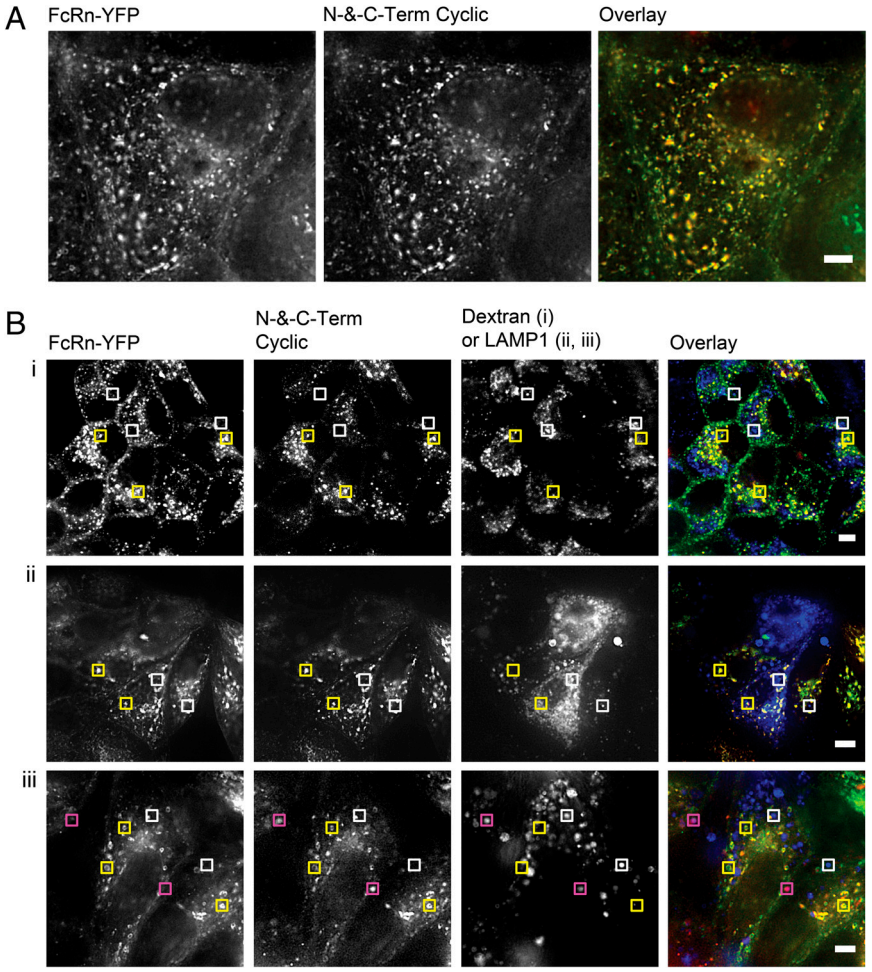

Fig. 3. Fluorescence Imaging of FcBP modified mKates in MDCK cells expressing hFcRn–EYFP. (*A*) Wide-field epifluorescence image of N-and-C-Term Cyclic FcBP mKate colocalization with hFcRn–EYFP in MDCK cells. Scale bar, 5 μm. (*B*, *i*) Confocal images of MDCK hFcRn–EYFP/hβ_2m cells showing the distribution of hFcRn–EYFP, N-and-C-Term Cyclic FcBP mKate, and 10 kDa dextran. (*B*, *ii* and *iii*) Wide-field epifluorescence images of MDCK hFcRn–EYFP/hβ_2m cells showing the distribution of hFcRn–EYFP, N-and-C-Term Cyclic FcBP mKate, and LAMP1-mTurquoise after 1-h (*ii*) or 4-h (*iii*) chase at 37 °C in HBSS, pH 7.4, prior to imaging. Yellow boxes indicate areas of colocalization between N-and-C-Term Cyclic FcBP mKate and FcRn–EYFP; white boxes indicate LAMP1-mTurquoise compartments that do not contain N-and-C-Term Cyclic FcBP mKate or FcRn–EYFP; and pink boxes indicate areas of colocalization between N-and-C-Term Cyclic FcBP mKate and LAMP1-mTurquoise. Scale bars: (*i*) 10 μm; (*ii* and *iii*) 5 μm. The overlays are pseudocolored as follows: Green indicates hFcRn–EYFP; red indicates N-and-C-Term Cyclic FcBP mKate; blue indicates dextran or LAMP1-mTurquoise; yellow indicates colocalization between FcRn and N-and-C-Term Cyclic FcBP mKate; and pink indicates colocalization between N-and-C-Term Cyclic FcBP mKate and LAMP1.

to cross the MDCK cell barrier (Fig. 4*B*). Transcytosis of N-and-C-Term Cyclic FcBP mKate across MDCK hFcRn–EYFP/hβ_2m cells is dose-dependent, indicating a FcRn-dependent transcytosis process (Fig. S8). Transcytosis of all proteins across MDCK cells lacking FcRn is undetectable, indicating that FcRn is necessary to deliver proteins across the MDCK epithelial cell barrier. Transport of the paracellular probe FITC-inulin was similar across transwells (Fig. S9), indicating that a tight, uniform barrier formed between the apical and basolateral chambers, and that differences in transport between proteins were mediated by FcRn.

Tyr12 to His FcBP Mutant with Altered Affinity for FcRn. Using a rational-design approach we identified a simple point mutation (Tyr-12 to His) in the FcBP sequence that improves pH-dependent binding to human FcRn (Table 1 and Fig. S10). Based on the crystal structure (25), the phenolic hydroxyl of Tyr-12 in the FcBP sequence makes an end-on-end hydrogen bond with Tyr-88 of FcRn, an interaction that likely contributes to binding at pH 7.4. We tested if mutation of Tyr-12 to His eliminates this hydrogen bond and creates a pH-dependent salt bridge between His and the nearby Glu-133 of FcRn (Fig. S10*B*). Indeed, mutation of the C-terminal FcBP Tyr to His of N-and-C-Term Cyclic FcBP mKate (Y286H variant) retains affinity and half-maximal uptake at pH 6 with little to no binding or cellular accumulation at pH 7.4 (Table 1 and Fig. S10*C*). We also evaluated the transport of the Y286H variant across MDCK hFcRn–EYFP/hβ_2m cell monolayers with both the apical and basolateral chambers equilibrated to pH 7.4, conditions that are more representative of the lung air and interstitial space. Significantly more ($P < 0.001$) N-and-C-Term Cyclic FcBP mKate was transported across the MDCK hFcRn–EYFP/hβ_2m cell monolayer compared to the Y286H variant (Fig. 4*C*). These findings support the hypothesis that low to moderate affinity at pH 7.4 for FcRn promotes transport across epithelial cell monolayers and may enhance systemic accumulation of pulmonary administered FcBP fusion proteins.

Discussion

In this study, we demonstrate that proteins can be engineered to interact with FcRn by recombinant fusion of a short FcBP sequence at a protein's N and/or C termini. This strategy is, to our knowledge, the only report of proteins engineered to interact with FcRn from non-Fc or albumin domains. Our strategy was motivated by results of Mezo et al. (20), who identified and

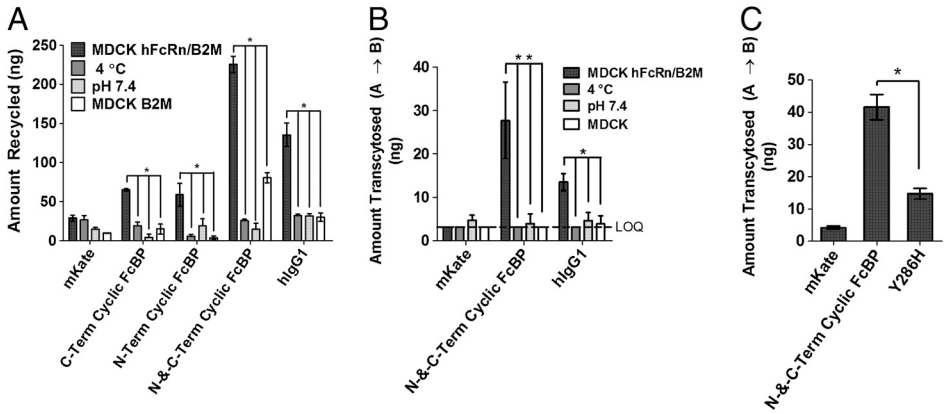

Fig. 4. FcBP fusion enables FcRn-mediated recycling and transcytosis. (*A*) In vitro FcRn-mediated recycling from MDCK hFcRn–EYFP/hβ_2m cells. Asterisk indicates significance with $P < 0.001$. (*B*) In vitro FcRn-mediated transcytosis across MDCK hFcRn–EYFP/hβ_2m or wild-type MDCK cell monolayers grown on transwell inserts. The data shown are the amount of protein transported to the basolateral compartment after a 2-h continuous incubation with 2.5 μM mKate or FcBP-modified mKates, and 1 μM labeled hIgG1 in the apical compartment. The apical chamber was equilibrated to pH 6, unless noted, and the basolateral to pH 7.4 in all cases. Double asterisks indicate that transcytosis is statistically significant between the specified groups, with $P < 0.001$. Single asterisk indicates significance with $P < 0.01$. Transport below the limit of quantification (LOQ) is indicated by the dashed line at 3.1 ng. (*C*) Transcytosis of 5 μM mKate or FcBP-modified mKates in the apical to basolateral direction after a 5-h continuous incubation at 37 °C with both compartments equilibrated to pH 7.4. Asterisk indicates significance with $P < 0.001$. The data shown for each panel are the mean ($n = 3$), and error bars indicate SD.

engineered peptides that compete with IgG for binding to FcRn as potential therapeutics for the treatment of IgG-mediated autoimmune disease. We built upon the Mezo approach and hypothesized that the phage-identified peptide sequence would be an ideal ligand for genetically engineering proteins to interact with FcRn for a number of reasons. First, the identified FcBPs exhibited binding to FcRn at pH 6 with a significant reduction in binding at pH 7.4, a critical property for FcRn-mediated protection from lysosomal degradation. Second, peptide dimerization resulted in a dramatic increase in affinity, which, based on the crystal structure, was caused by avidity from a 2:1 interaction with FcRn (25). Third, the small size and simple structure of the FcBP would enable expression of FcBP fusions in *E. coli*. Finally, a recombinant peptide tag that improves protein pharmacokinetics and delivery may overcome limitations associated with protein–polymer conjugates and Fc or albumin fusion, which significantly increases molecular weight and decreases biological activity and tissue penetration.

A family of FcBP fusion proteins were engineered and characterized using molecular and cell-based assays. FcBP fusion at the N and/or C termini of mKate results in a pH-dependent interaction with FcRn that is modulated by altering the FcBP sequence or number of FcBPs fused to the protein. A majority of FcRn-binding and -trafficking properties are similar between IgG and FcBP fusions; however, a difference occurs at pH 7.4. IgG has no appreciable FcRn-mediated cellular accumulation in FcRn-expressing MDCK cells at pH 7.4 or detectable binding by SPR, whereas significant accumulation and binding of N-and-C-Term Cyclic FcBP mKate occurs. Therefore, we rationally designed a Y286H variant of N-and-C-Term Cyclic FcBP mKate with negligible binding to FcRn at pH 7.4 to probe the role of affinity at pH 7.4 on FcRn transport.

There have been a number of reports on the relationship between affinity for FcRn at physiological pH and in vivo circulation time (26–28). In general, variant IgGs with appreciable affinity for FcRn at physiological pH have reduced circulation time and increased clearance compared to wild-type IgG, likely because of catabolism of variant IgGs that do not dissociate from FcRn during receptor turnover. However, moderate affinity for FcRn at pH 7.4 may be advantageous for low-molecular weight proteins that exhibit rapid renal clearance. This affinity may promote salvage of FcBP fusion proteins by FcRn expressed in renal proximal tubule cells (29), resulting in reabsorption of intact protein filtered through the glomerulus. Similarly, moderate affinity at physiological pH may improve absorption of FcBP fusion proteins from the lung airway by FcRn expressed on the apical surface of bronchial epithelial cells (12). Indeed, we found that N-and-C-Term Cyclic FcBP mKate was transported to a greater extent than the Y286H variant across FcRn-expressing MDCK cell monolayers. Additional modifications that generate FcBP fusion proteins with differential FcRn-binding properties will provide interesting tools to probe further the biology of FcRn related to protein drug delivery.

In summary, our results demonstrate that proteins can be engineered to interact with FcRn from non-IgG domains based on a simple recombinant fusion to a small polypeptide resulting in protein mimetics of the IgG:FcRn interaction. These findings suggest that FcBP fusion may be an effective strategy to improve protein pharmacokinetics and/or delivery—a strategy that is applicable to a wide range of rapidly eliminated protein therapeutics, such as a number of clinically relevant cytokines (IFNα2, IFNγ, TSG-6), hormones (hGH), and growth factors (EPO, GCSF-3) whose termini are not involved in receptor binding (30), or next-generation protein therapeutics including small antibody fragment and engineered protein scaffolds. Additional in vivo studies are necessary, however, to realize fully the potential of the FcBP fusion platform. In addition, this strategy may be applicable to alternative systems including liposomes, polymers, dendrimers, nucleic acids, viruses, or small molecules as a means to improve drug delivery by targeting FcRn.

Materials and Methods

Affinity Measurements by Surface Plasmon Resonance. SPR measurements were obtained using a BIAcore T100 instrument (BIAcore Inc.). The extracellular region of human FcRn (a kind gift of E. Sally Ward, University of Texas Southwestern Medical Center, Dallas, TX) was captured on a CM5 sensor chip at pH 5 by amine coupling to a final immobilization density of approximately 550 or approximately 100 resonance units. Unreacted sites were blocked with 1 M ethanolamine. A control flow cell without immobilized hFcRn was prepared for reference subtraction. All binding experiments were preformed as previously described for the synthetic FcBP (20) with the following modifications: The flow rate used for all methods was 30 μL/min and injection times were 60 s. Proteins were dissociated from the chip for 45 s in running buffer followed by regeneration with 45-s injections of HBS-P (10 mM Hepes, 150 mM NaCl, 0.005% Tween 20, pH 7.4) and/or Tris, pH 9 buffer (50 mM Tris, 100 mM NaCl, 0.01% Tween 20, pH 9). Binding kinetics were derived by analysis of the generated sensograms using the BIAcore T100 evaluation software. Sensograms were fit to a 1:1 binding model included in the evaluation software.

FACS Cellular Accumulation Assay. Because of the far-red fluorescent properties of mKate (Ex/Em: 588/635), cell-associated FcBP-modified mKate can be quantified via FACS. MDCK hFcRn–EYFP/hβ_2m cells were washed twice in binding buffer (HBSS, 1% ovalbumin, 50 mM MES, pH 6) and incubated with serial dilutions of proteins for 1 h at 37 °C to permit cellular uptake. Cells were washed twice with cold binding buffer to remove unbound protein, trypsinized, and analyzed on a FACS-array cell sorter (BD Biosciences). MFIs for each test population were derived after gating for live and EYFP-positive cells. Binding at pH 7.4 was as described above, except all incubations and washes were done in HBSS(+), pH 7.4 (HBSS, 1% ovalbumin, 50 mM HEPES, pH 7.4). Protein accumulation in MDCK hβ_2m, wild-type MDCK, and B16F10 cells at pH 6 was as described above. All FACS data were analyzed using FlowJo (Tree Star Inc.). All incubations were done in triplicate and data are represented as mean ± SD.

FcRn-Mediated Recycling and Transcytosis Assay. FcRn-mediated recycling and transcytosis were assessed as previously described for Fc domains (18), with minor modifications. Recycling was assessed on nonpolarized MDCK hFcRn–EYFP/hβ_2m or MDCKhβ_2m cells pulsed with 2.5 μM of mKate, 2.5 μM mKates modified with a single FcBP, 1 μM mKate modified at both termini, or 1 μM labeled hIgG1 for 1 h at 37 °C in binding buffer to permit uptake. Cells were washed four times with cold HBSS(+), pH 8.5 (HBSS, 1% ovalbumin, 50 mM Tris, pH 8.5), to remove surface-bound protein and chased with prewarmed HBSS(+), pH 7.4, for 2 h at 37 °C. The media containing recycled proteins were collected, centrifuged to remove dead or detached cells. The amount of protein in the supernatant was then quantified by fluorometry. Controls (including recycling at 4 °C, pH 7.4, and in hFcRn-negative MDCK cells) were conducted as described above with the appropriate modification.

FcRn-mediated transcytosis was assessed across polarized wild-type MDCK or MDCK hFcRn–EYFP/hβ_2m cell monolayers cultured on transwell filters (12-mm diameter, 0.4-μm pore size; Corning Life Sciences). Wild-type MDCK cells were used as controls because they formed polarized monolayers whereas MDCK hβ_2m cells did not form monolayers. Cell confluence was confirmed by a transepithelial electrical resistance (TEER) greater than 250 Ω/cm^2 prior to experiments typically conduced 4 days after initial cell seeding. Apical-to-basolateral transcytosis was measured by incubating the apical chamber with 0.5 mL of 2.5 μM of mKate, 2.5 μM N-and-C-Term Cyclic FcBP mKate, or 0.5 μM labeled hIgG1 in HBSS(+), pH 6 or pH 7.4, and the basolateral chamber with 1 mL of HBSS(+), pH 7.4. FITC-inulin (4 μg/mL) was coincubated with protein in the apical compartment as a marker for paracellular transport and monolayer consistency across transwells. The amount of protein and FITC-inulin transported to the basolateral chamber after a 2-h continuous incubation at 37 °C or 4 °C was quantified by fluorometry.

ACKNOWLEDGMENTS. We thank L. Kohlstaedt and the University of California, Berkeley, Proteomics/Mass Spectrometry Laboratory for LC–MS/MS analysis; K. Thorn and A. Myo Thwin at the University of California, San Francisco, Nikon Imaging Center; S. Peck and J. Wong at the University of California, San Francisco, Biological Imaging and Development Center; P. Hwang and V. Venditto for assistance with SPR; and E. S. Ward and U. Bussmeyer at University of Texas Southwestern Medical Center for critical reagents. This work is funded in part by National Institutes of Health Grants 1 R21 EB015520-01 and TG T32 GM007175. J.S. acknowledges past and current support from the American Foundation for Pharmaceutical Education (AFPE), University of California, San Francisco, Graduate Dean's Chancellor's Fellowship, and the Pharmaceutical Research and Manufacturers of America (PhRMA) foundation.

1. Kontermann RE (2011) Strategies for extended serum half-life of protein therapeutics. *Curr Opin Biotechnol* 22:868–876.
2. Wang W, Wang EQ, Balthasar JP (2008) Monoclonal antibody pharmacokinetics and pharmacodynamics. *Clin Pharmacol Ther* 84:548–558.
3. Roopenian DC, Akilesh S (2007) FcRn: The neonatal Fc receptor comes of age. *Nat Rev Immunol* 7:715–725.
4. Abuchowski A, McCoy JR, Palczuk NC, van Es T, Davis FF (1977) Effect of covalent attachment of polyethylene glycol on immunogenicity and circulating life of bovine liver catalase. *J Biol Chem* 252:3582–3586.
5. Alconcel SNS, Baas AS, Maynard HD (2011) FDA-approved poly(ethylene glycol)–protein conjugate drugs. *Polymer Chem* 2:1442–1448.
6. Gao W, Liu W, Christensen T, Zalutsky MR, Chilkoti A (2010) In situ growth of a PEG-like polymer from the C terminus of an intein fusion protein improves pharmacokinetics and tumor accumulation. *Proc Natl Acad Sci USA* 107:16432–16437.
7. Schellenberger V, et al. (2009) A recombinant polypeptide extends the in vivo half-life of peptides and proteins in a tunable manner. *Nat Biotechnol* 27:1186–1190.
8. Vallee S, et al. (2011) Pulmonary administration of interferon beta-1a-Fc fusion protein in non-human primates using an immunoglobulin transport pathway. *J Interferon Cytokine Res* 32:178–184.
9. Gong R, Wang Y, Feng Y, Zhao Q, Dimitrov DS (2011) Shortened engineered human antibody CH2 domains: Increased stability and binding to the human neonatal Fc receptor. *J Biol Chem* 286:27288–27293.
10. Ying T, Chen W, Gong R, Feng Y, Dimitrov DS (2012) Soluble monomeric IgG1 Fc. *J Biol Chem* 287:19399–19408.
11. Andersen JT, et al. (2011) Extending half-life by indirect targeting of the neonatal Fc receptor (FcRn) using a minimal albumin binding domain. *J Biol Chem* 286:5234–5241.
12. Spiekermann GM, et al. (2002) Receptor-mediated immunoglobulin G transport across mucosal barriers in adult life: Functional expression of FcRn in the mammalian lung. *J Exp Med* 196:303–310.
13. Amet N, Wang W, Shen W-C (2010) Human growth hormone-transferrin fusion protein for oral delivery in hypophysectomized rats. *J Control Release* 141:177–182.
14. Dumont JA, et al. (2005) Delivery of an erythropoietin-Fc fusion protein by inhalation in humans through an immunoglobulin transport pathway. *J Aerosol Med* 18:294–303.
15. Patton JS, Byron PR (2007) Inhaling medicines: Delivering drugs to the body through the lungs. *Nat Rev Drug Discov* 6:67–74.
16. Shcherbo D, et al. (2007) Bright far-red fluorescent protein for whole-body imaging. *Nat Methods* 4:741–746.
17. West AP, Bjorkman PJ (2000) Crystal structure and immunoglobulin G binding properties of the human major histocompatibility complex-related Fc receptor. *Biochemistry* 39:9698–9708.
18. Tesar DB, Tiangco NE, Bjorkman PJ (2006) Ligand valency affects transcytosis, recycling and intracellular trafficking mediated by the neonatal Fc receptor. *Traffic* 7:1127–1142.
19. Kim JK, Tsen MF, Ghetie V, Ward ES (1994) Catabolism of the murine IgG1 molecule: Evidence that both CH2-CH3 domain interfaces are required for persistence of IgG1 in the circulation of mice. *Scand J Immunol* 40:457–465.
20. Mezo AR, et al. (2008) Reduction of IgG in nonhuman primates by a peptide antagonist of the neonatal Fc receptor FcRn. *Proc Natl Acad Sci USA* 105:2337–2342.
21. Tesar DB, Björkman PJ (2010) An intracellular traffic jam: Fc receptor-mediated transport of immunoglobulin G. *Curr Opin Struct Biol* 20:226–233.
22. Ober RJ, Martinez C, Vaccaro C, Zhou J, Ward ES (2004) Visualizing the site and dynamics of IgG salvage by the MHC class I-related receptor, FcRn. *J Immunol* 172:2021–2029.
23. Prabhat P, et al. (2007) Elucidation of intracellular recycling pathways leading to exocytosis of the Fc receptor, FcRn, by using multifocal plane microscopy. *Proc Natl Acad Sci USA* 104:5889–5894.
24. Gan Z, Ram S, Vaccaro C, Ober RJ, Ward ES (2009) Analyses of the recycling receptor, FcRn, in live cells reveal novel pathways for lysosomal delivery. *Traffic* 10:600–614.
25. Mezo AR, Sridhar V, Badger J, Sakorafas P, Nienaber V (2010) X-ray crystal structures of monomeric and dimeric peptide inhibitors in complex with the human neonatal Fc receptor, FcRn. *J Biol Chem* 285:27694–27701.
26. Yeung YA, et al. (2009) Engineering human IgG1 affinity to human neonatal Fc receptor: Impact of affinity improvement on pharmacokinetics in primates. *J Immunol* 182:7663–7671.
27. Yeung YA, et al. (2010) A therapeutic anti-VEGF antibody with increased potency independent of pharmacokinetic half-life. *Cancer Res* 70:3269–3277.
28. Acqua WFD, et al. (2002) Increasing the affinity of a human IgG1 for the neonatal Fc receptor: Biological consequences. *J Immunol* 169:5171–5180.
29. Kobayashi N, et al. (2002) FcRn-mediated transcytosis of immunoglobulin G in human renal proximal tubular epithelial cells. *Am J Physiol Renal Physiol* 282:F358–F365.
30. Wang X, Lupardus P, Laporte SL, Garcia KC (2009) Structural biology of shared cytokine receptors. *Annu Rev Immunol* 27:29–60.